The place of the Local Group in the cosmic web

Jaime E. Forero-Romero[1] and Roberto González[2,3]

[1]Departamento de Física, Universidad de los Andes,
Cra. 1 No. 18A-10, Edificio Ip
Bogotá, Colombia
email: `je.forero@uniandes.edu.co`

[2]Instituto de Astrofísica, Pontificia Universidad Católica de Chile
Av. Vicuña Mackenna 4860
Santiago, Chile

[3]Centro de Astro-Ingeniería, Pontificia Universidad Católica de Chile
Av. Vicuña Mackenna 4860
Santiago, Chile
email: `regonzar@astro.puc.cl`

Abstract. We use the Bolshoi Simulation to find the most probable location of the Local Group (LG) in the cosmic web. Our LG simulacra are pairs of halos with isolation and kinematic properties consistent with observations. The cosmic web is defined using a tidal tensor approach. We find that the LG's preferred location is regions with a dark matter overdensity close to the cosmic average. This makes filaments and sheets the preferred environment. We also find a strong alignment between the LG and the cosmic web. The orbital angular momentum is preferentially perpendicular to the smallest tidal eigenvector, while the vector connecting the two halos is strongly aligned along the the smallest tidal eigenvector and perpendicular to the largest tidal eigenvector; the pair lies and moves along filaments and sheets. We do not find any evidence for an alignment between the spin of each halo in the pair and the cosmic web.

Keywords. cosmology: large-scale structure of universe; cosmology:dark matter; cosmology: simulations; Galaxy: formation

1. Introduction

The kinematic configuration of the Local Group (LG) is not common in the cosmological context provided by the Λ Cold Dark Matter (CDM) model.

The LG is dominated by the presence of two spiral galaxies, the Milky Way (MW) and M31. It is relatively isolated of other massive structures; the next most luminous galaxy is 10 times less massive than M31, with several dwarf galaxies around a sphere of ~ 3Mpc and the closest massive galaxy cluster, the Virgo Cluster, is 16.5 Mpc away. The velocity vector of M31 has a low tangential component and is consistent with a head-on collision toward the MW, and the velocity dispersion of nearby galaxies up to ~ 8 Mpc is relatively low.

These features make LG analogues uncommon in numerical simulations. Only about of 2% of MW-sized halos reside in a pair similar to the MW-M31 in a similar environment. Additionally, the strong alignments of dwarf satellites of the MW and M31 in the form of polar and planar structures calls asks for a detailed explanation of the large scale structure environment that can breed such halos (González & Padilla(2010), González *et al.* (2014), González *et al.* (2013), Forero-Romero *et al.* (2011), Forero-Romero *et al.* (2013)).

Here we present results of the study of the large scale environment of LG analogues in the context of ΛCDM. We use a cosmological N-body simulation (Bolshoi) to infer the most probable place of the LG in the cosmic web and its alignments. A detailed description of these results can found in Forero-Romero & González (2014).

2. Finding the cosmic web in numerical simulations

We use a web finding algorithm based on the tidal tensor computed from the gravitational potential field computed over a grid. We define the tensor as:

$$T_{ij} = \frac{\partial^2 \phi}{\partial r_i \partial r_j}, \tag{2.1}$$

where the index $i = 1, 2, 3$ refers to the three spatial directions in euclidean space and ϕ is a normalized gravitational potential that satisfies the following Poisson equation $\nabla^2 \phi = \delta$, where δ is the dark matter overdensity.

The algorithm finds the eigenvalues of this tensor, $\lambda_1 > \lambda_2 > \lambda_3$, and use them to classify each cell in the grid as a peak, filament, sheet or void if three, two, one or none of the eigenvectors is larger than a given threshold λ_{th}. Each eigenvalue has associated to it an eigenvector (e_1, e_2, e_3) which are the natural basis to define local directions in the web. Details describing the algorithm can be found in Forero-Romero et $al.$ (2009). The dark matter density is interpolated over a grid with cells of size $0.97\ h^{-1}$Mpc and smoothed with a Gaussian filter with the same spatial scale. We use a threshold of $\lambda_{th} = 0.25$ to define the different cosmic web environments.

We use the Bolshoi simulation with a ΛCDM cosmology described by the parameters $\Omega_{\mathrm{m}} = 1 - \Omega_{\Lambda} = 0.27$, $H_0 = 70\,\mathrm{km/s/Mpc}$, $\sigma_8 = 0.82$, $n_s = 0.95$ (Klypin et $al.$ (2011)). The simulation followed the evolution of dark matter in a $250 h^{-1}$Mpc box with spatial resolution of $\approx 1 h^{-1}$ kpc and mass resolution of $m_{\mathrm{p}} = 1.35 \times 10^8$ M$_\odot$. Halos are identified with the Bound Density Maxima (BDM) algorithm (Klypin & Holtzman(1997)). The data for the halos and the cosmic web are available through a public database located at `http://www.cosmosim.org/`. A detailed description of the database structure was presented by Riebe et $al.$ (2013).

3. Local Groups in cosmological simulations

We construct a sample of MW-M31 pairs at $z \sim 0$ by using multiple snapshots from the simulation asking for consistency with the following criteria:

• Relative distance. The distance between the center of mass of each halo in the pair cannot be larger than 1.3 Mpc.

• Individual halo mass. Each halo has a mass in the mass range $5 \times 10^{11} < M_{200c} < 5 \times 10^{13}M_\odot$.

• Isolation. No neighboring halos more massive than either pair member can be found within 5Mpc.

• Isolation from Virgo-like halos. No dark matter halos with mass $M_{200c} > 1.5 \times 10^{14}M_\odot$ within 12Mpc.

With these selection criteria we select close to 6×10^3 pairs to build a General Sample (GS). From the GS we select two sub-samples according to the tolerance in kinematic constraints. These sub-samples are named 2σ and 3σ, they correspond to a tolerance of two and three times the observational errors in the radial velocity, tangential velocity and separation. The number of pairs in each sample is 46 and 120, respectively.
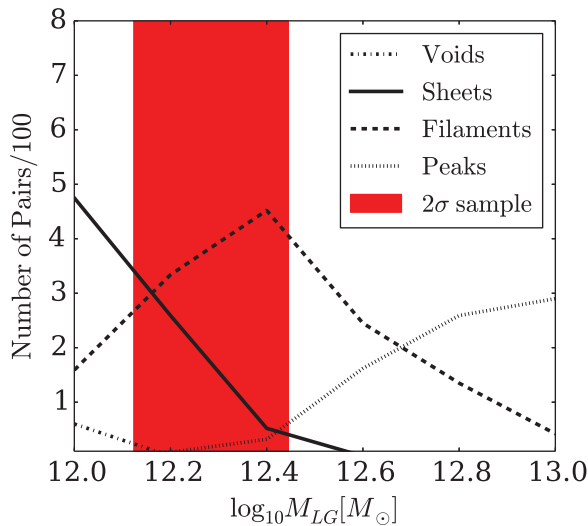
Figure 1. Number of pairs in a preferred environment as a function of the LG total mass. The lines show the results for the General Sample, the shaded region shows the mass interval spanned by the 2σ sample. The preferred environments are filaments and sheets.

4. The place of the Local Group in the Cosmic Web

We find that the pairs in the general sample are located across different environments with a strong dependence on the total pair mass. Figure 1 summarizes this correlation between environment and mass. Each line represents the distribution of pairs in the four different environments. High mass pairs are mostly located in peaks and filaments while less massive ones in voids and sheets. The shaded regions represent the 68% confidence intervals of the mass distributions in the 2σ sample. By and large the LGs in the 2σ and 3σ samples are located in filaments and sheets. In both samples, $\sim 50\%$ of the pairs can be found in filaments while $\sim 40\%$ are in sheets.

We can also characterize the preferred place of the pair samples in terms of the web overdensity. Figure 2 shows the values of the overdensity as a function of the total pair mass. The GS and its uncertainties are represented by the shaded region. The symbols represent the results for the 2σ and 3σ samples. We see that the range of values for the restricted samples samples are completely expected from the mass constraint alone. Higher mass pairs are located in high density regions. The 2σ and 3σ samples have narrower mass range and are located within a narrower range of overdensities $0.0 < \delta < 2.0$ peaking at $\delta \sim 1$.

5. Alignments with the cosmic web

There is wide evidence showing that DM halo formation properties only depend on environment through the local DM density. Whether they are located in sheet or a filament is irrelevant as long the local density is the same.

However there is long history of alignment measurement (shape, spin, peculiar velocities) of individual halos with the cosmic web. In a recent paper Forero-Romero *et al.* (2014) presented a study using the same simulation and cosmic web definition we use here. They also presented a comprehensive review of all the previous results from simulations that also inspected the alignment of halo shape and spin. We refer the reader to the paper for a complete list of references.
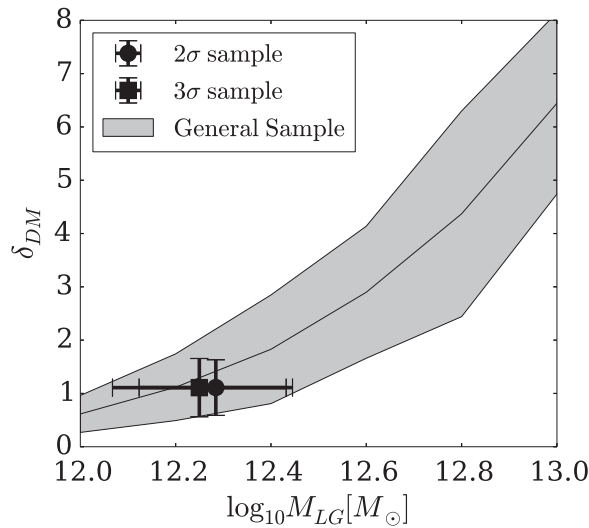
Figure 2. Dark matter overdensity as a function of the LG total mass. The shaded region show the results for the General Sample. There is a strong correlation where more massive pairs sit in denser regions. The symbols represent the 2σ and 3σ samples. The preferred overdensity is in the interval $0 < \delta < 2$.
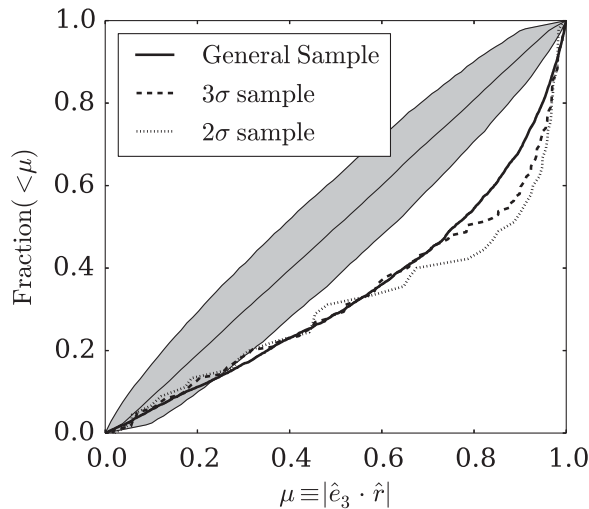

Figure 3. Cumulative distribution for $\mu = |\hat{e}_3 \cdot \hat{r}|$ showing the alignment of the vector joining the two halos in the LG with the smallest tidal eigenvector. The shaded regions represents the expected result from a distribution of vectors randomly placed in space and the corresponding 5% and 75% percentiles for distributions with the same number of points as the 2σ sample.

The main results from the study in Forero-Romero *et al.* (2014) is that the halo shape presents the strongest alignment signal. In this case the DM halo major axis lies along the smallest eigenvector e_3, regardless of the web environment. This alignments is stronger for higher halo masses. Concerning spin alignment the simulations show a weak anti-alignment with respect to e_3 for halo masses larger that $10^{12} M_\odot$, and no alignment signal for masses below that threshold. The peculiar velocities show a strong alignment signal along e_3 for all masses.
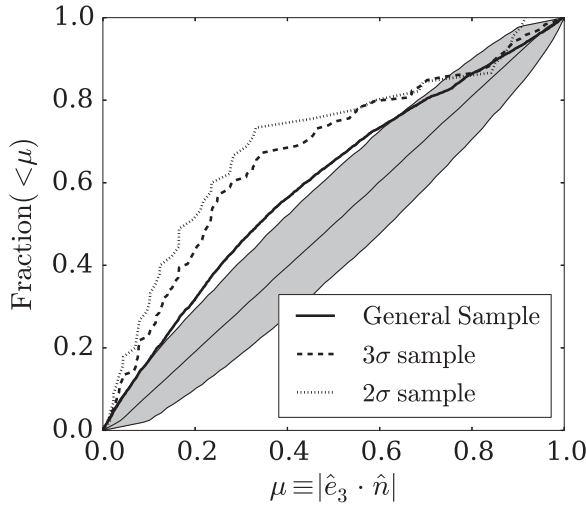
Figure 4. Same as Figure 3 for the vector $\hat{n}$ that indicates the direction of the orbital angular momentum of the pair.

In our case we test for the alignment of the vector connecting the two halos ($\hat{r}$), the orbital angular momentum of the pair ($\hat{n}$) and the spin of each halo. We quantify the alignment using the absolute value of the cosine of the angle between two vectors $\mu = |\hat{e}_3 \cdot \hat{n}|$ or $\mu = |\hat{e}_3 \cdot \hat{r}|$.

The results for the first two alignments are summarized in Figures 3 and 4. We find that the vector $\hat{r}$ is strongly aligned with $\hat{e}_3$, along filaments and sheets. This trend is already present in the GS and gets stronger for the 2σ and 3σ samples. Concerning the vector $\hat{n}$ we have a strong anti-correlation with $\hat{e}_3$, again this tendency is stronger for the 2σ and 3σ samples.

6. Conclusions

Here, we have presented results on the expected place of the Local Group in the cosmic web. Our results are based on cosmological N-body simulations and the tidal web method to define the cosmic web. We constructed different Local Groups samples from dark matter halo pairs that fulfill observational kinematic constraints.

We found a tight correlation of the LG pairs' total mass with the local overdensity. For the LG pairs closer to the observational constraints their total mass is in the range $1 \times 10^{12} \mathrm{M}_\odot < M_{LG} < 4 \times 10^{12} \mathrm{M}_\odot$ preferred overdensity value is constrained to be in the range $0 < \delta < 2$. This restricts the preferred environment to be filaments and sheets.

We also found strong alignments of the pairs with the cosmic web. The strongest alignment is present for the vector joining the two LG halos. This vector is aligned with the lowest eigenvector and anti-aligned with the highest eigenvector. This trend is already present in wide sample of pairs and becomes stronger as the kinematic constraints are closer to their observed values.

These results raise the need to use observations to constraint the alignments of LG pairs with their cosmic web environment. There are many algorithms available to reconstruct the DM distribution from large galaxy surveys to tackle this task. This would allow a direct quantification of how common are the LG alignments we have found, providing a potential new test for ΛCDM.

References

Forero-Romero, J. E., & González, R. E., *ApJ* accepted, ArXiv:1408.3166

Forero-Romero, J. E., Contreras, S., & Padilla, N. 2014, MNRAS, 443, 1090

Forero-Romero, J. E., Hoffman, Y., Bustamante, S., Gottlöber, S., & Yepes, G. 2013, ApJL, 767, L5

Forero-Romero, J. E., Hoffman, Y., Yepes, G., Gottlöber, S., Piontek, R., Klypin, A., & Steinmetz, M. 2011, MNRAS, 417, 1434

Forero-Romero, J. E., Hoffman, Y., Gottlöber, S., Klypin, A., & Yepes, G. 2009, MNRAS, 396, 1815

González, R. E., Kravtsov, A. V., & Gnedin, N. Y. 2013, ApJ, 770, 96

—, 2014, ApJ, 793, 91

González, R. E. & Padilla, N. D. 2010, MNRAS, 407, 1449

Hoffman Y., Metuki O., Yepes G., Gottlöber S., Forero-Romero J. E., Libeskind N. I., Knebe A., 2012, MNRAS, 425, 2049

Klypin, A. A., Trujillo-Gomez, S., & Primack, J. 2011, ApJ, 740, 102

Klypin, A. & Holtzman, J. 1997, ArXiv:9712217

Riebe, K., Partl, A. M., Enke, H., Forero-Romero, J., Gottlöber, S., Klypin, A., Lemson, G., Prada, F., Primack, J. R., Steinmetz, M., & Turchaninov, V. 2013, *Astronomische Nachrichten*, 334, 691